

Fluorescence Spectra for the Microcrystals and Thin Films of *trans,trans,trans*-1,6-Diphenyl-1,3,5-hexatrienes

Yoriko Sonoda,^{*,†} Yuji Kawanishi,[†] Takuji Ikeda,^{‡,§} Midori Goto,^{||} Shigenobu Hayashi,[⊥] Yuji Yoshida,[#] Nobutaka Tanigaki,[#] and Kiyoshi Yase[#]

Nanotechnology Research Institute, Technical Center, Institute for Materials and Chemical Process, and Photonics Research Institute, National Institute of Advanced Industrial Science and Technology (AIST), Higashi 1-1-1, Tsukuba, Ibaraki 305-8565, Japan; and Advanced Materials Laboratory, National Institute for Materials Science, 1-1 Namiki, Tsukuba, Ibaraki 305-0044, Japan

Received: August 6, 2002; In Final Form: December 2, 2002

The absorption and fluorescence spectra, fluorescence quantum yields (ϕ_{flu}), and lifetimes (τ_s) for the microcrystals and vacuum deposited thin films of the *p,p'*-disubstituted *trans,trans,trans*-1,6-diphenyl-1,3,5-hexatrienes (DPHs) **1–10** have been measured and compared with those in dilute solutions at room temperature and in organic glasses at 77 K. The positions of the peaks at the shortest wavelengths in the fluorescence main bands, which are mainly determined by effective π -conjugation lengths (ECLs) in the excited state, are tuned in the visible spectral range 463–587 nm by introduction of various substituents. The fluorescence main bands shift to longer wavelengths as the strength of electron-donating/withdrawing substituents on the aromatic ring increases. The fluorescence spectra of the microcrystalline samples are more strongly dependent on substituents than those of samples in solution, because of strong charge transfer (CT) type intermolecular interactions induced by substituents in the solid state. The solid-state fluorescence spectra of the derivatives with electron-donating *N,N*-dimethylamino and methoxy groups (**1** and **2**, respectively) are red-shifted and structured, probably due to the formation of ground-state aggregates. The spectrum for the thin film of **2** shows a close resemblance to that for the thin film of high molecular weight poly(1,4-phenylenevinylene) (PPV), suggesting similar ECLs for **2** and PPV in the excited states. The spectra of the derivatives with electron-withdrawing substituents, on the other hand, are red-shifted and structureless. The broad fluorescence observed for the diformyl derivative (**6**) is assigned to excimer emission.

Introduction

trans,trans,trans-1,6-Diphenyl-1,3,5-hexatriene [*trans,trans,trans*-DPH] (**4**) is widely used for biological and membrane studies because of its fluorescence anisotropies.¹ The emission properties of DPH and its derivatives in solution have been extensively studied because of its unique fluorescence behavior. DPH is known to exhibit dual fluorescence from S_1 and S_2 at thermal equilibrium.² In addition to the spectroscopic studies, the photochemical reactions such as *cis-trans*-isomerization have attracted considerable attention,^{3–5} due to the structural similarity of DPH to visual pigments. For the solid-state photoreactivities of DPHs, we have recently shown that the formyl (**6**) and cyano (**9**) derivatives undergo [2 + 2] photocycloadditions to give dimers (and oligomers for **9**).⁶ However, the emission properties of DPHs in the solid state are not known at present.

The solid-state fluorescence of π -conjugated polymers and oligomers has attracted a considerable amount of attention

recently, due to their applications in electroluminescence (EL) devices. A dialkoxy-substituted PPV with cyano groups on the vinylene units shows red-shifted fluorescence and improved emission efficiency relative to those for the unsubstituted polymer.⁷ Optical properties of oligo-phenylenevinylenes (oligo-PVs) and oligo-thiophenes have also been extensively studied both experimentally^{8–14} and theoretically.^{15,16} For these oligomers, the absorption and fluorescence properties are highly dependent on molecular orientation.^{8–10,13–15} On the other hand, it is found that substitution with alkoxy and cyano groups on the benzene ring and ethylene bond, respectively, is effective to reduce the HOMO–LUMO band gaps of PV oligomers.^{8,12,16} Knowledge about emission properties of conjugated compounds in various solid states is of great importance for a better understanding of π -electron delocalization between fluorescent molecules in supramolecular structures.

Since DPHs have rodlike molecular structures, it is expected that the emission properties in the solid state are strongly affected by intermolecular interactions and molecular arrangements. In this study, absorption and fluorescence spectra, fluorescence quantum yields (ϕ_{flu}), and lifetimes (τ_s) for the microcrystals and vacuum deposited thin films of DPHs **1–10** were investigated. It was shown that the solid-state fluorescence compared to solution was more strongly dependent on substituents. The emission properties of the solid-state DPHs were very similar to those for the ordered solid phases of PV oligomers.

* To whom correspondence should be addressed. Fax: +81-298-61-6296. E-mail: y.sonoda@aist.go.jp.

[†] Nanotechnology Research Institute, National Institute of Advanced Industrial Science and Technology (AIST).

[‡] Present Address: Laboratory for Membrane Chemistry, AIST Tohoku, Sendai, Miyagi 983-8551, Japan.

[§] Advanced Materials Laboratory, National Institute for Materials Science.
^{||} Technical Center, National Institute of Advanced Industrial Science and Technology (AIST).

[⊥] Institute for Materials and Chemical Process, National Institute of Advanced Industrial Science and Technology (AIST).

[#] Photonics Research Institute, National Institute of Advanced Industrial Science and Technology (AIST).

Experimental Section

Materials. All solvents for preparing solutions were of UV spectroscopic grade (Dojin Kagaku) and used without further purification. Pyrene crystals (optical grade) used for the solid-state ϕ_{flu} measurements were purchased from Fluka and used as received.

The unsubstituted compound **4** (scintillation grade) was purchased from WAKO Pure Chemicals. The other DPH derivatives were prepared by Wittig reaction according to the literature.¹⁷ All DPH compounds were purified by recrystallization from appropriate solvents, and sample purity was checked by HPLC. The *trans,trans,trans* structure was confirmed by IR, ¹H NMR, and UV-vis spectroscopy. High molecular weight PPV was prepared by the sulfonium salt pyrolysis method.¹⁸

The crystalline powder of **6** used for synchrotron X-ray powder diffraction was obtained by very slow evaporation of solvent chloroform from a highly diluted solution in the dark at room temperature.

General Procedures. Absorption spectra were recorded on a Hitachi U-3210 spectrometer or a JASCO V-560. Corrected fluorescence and excitation spectra were recorded using a SPEX Fluorolog-3 spectrometer. Fluorescence decay curves were measured by the time-correlated single photon counting method, using a HORIBA NAES 700 equipped with a subnanosecond nitrogen-dye laser system. For fluorescence measurements, the excitation wavelength was 420 nm for **1** and **10**, 360 nm for **3–5**, and 375 nm for the other DPH derivatives and PPV, unless otherwise noted. Diluted samples ($<1.5 \times 10^{-6}$ M, <0.1 OD at the excitation wavelength) were used for the measurements in solution. Values of ϕ_{flu} in solution were determined using a solution of **9** in toluene as a standard ($\phi_{\text{flu}} = 0.88$).⁵ Fluorescence spectra in microcrystals and thin films were recorded by using front face geometry. Values of ϕ_{flu} in the solid state were estimated by comparison of fluorescence peak areas for the thick microcrystalline powder of the samples with that for pyrene ($\phi_{\text{flu}} = 0.64$ at 293 K).¹⁹

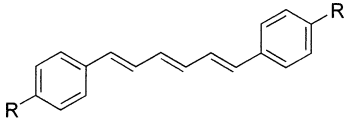
The sample microcrystals were placed between quartz plates ($40 \times 10 \text{ mm}^2$) to measure the optical spectra. The thin film of PPV was prepared on a quartz plate by the friction transferred method.

¹H NMR spectra in solution were recorded on a Varian Gemini-300 BB spectrometer (300.0 MHz) with tetramethylsilane (TMS) as internal standard. IR spectra were measured using a Perkin-Elmer PARAGON 1000 FT-IR spectrometer.

High-resolution solid-state NMR spectra of **2** and **6** were obtained with a Bruker ASX200 spectrometer, operating at ¹³C and ¹H resonance frequencies of 50.3 and 200.1 MHz, respectively. The ¹³C spectra were measured with a cross polarization technique (CP) under magic-angle spinning (MAS) of the sample. The samples were packed into zirconia rotors with outer diameters of 7 mm and were spun at 2.0–4.25 kHz. The ¹H spectra were obtained using the CRAMPS technique, where the BR-24 multipulse sequence was used with a quadrature detection mode.²⁰ The spinning rate was set at 1.6 kHz. Two-dimensional (2D) ¹H exchange spectra were measured with a pulse sequence similar to that in the literature,²¹ where the quadrature mode of BR-24 was used instead of that of MREV-8. The ¹³C and ¹H spectra were expressed with respect to pure TMS, with the higher frequency side being positive.

Synchrotron X-ray powder diffraction data (XRD) of **6** were collected at room temperature by using a high resolution powder diffractometer with the Debye–Scherrer geometry constructed at beam line BL15XU in the synchrotron radiation facility

TABLE 1: Absorption and Emission Properties of Diphenylhexatrienes in Toluene Solution



1 R = NMe₂

2 OMe

3 Me

4 H

5 Cl

6 CHO

7 COOH

8 COOMe

9 CN

10 NO₂

compd	R =	λ_{abs} (nm)	λ_{em} (nm)	ϕ_{flu}
1	NMe ₂	410	481	0.71
2	OMe	372	435	0.74
3	Me	364	433	0.66
4	H	359	428	0.74
5	Cl	366	436	0.71
6	CHO	395	464	0.76
7	COOH	372 ^a	443 ^a	0.065 ^a
8	COOMe	382	449	0.84
9	CN	380	452	0.88
10	NO ₂	410	491	0.10

^a Measured in methanol for solubility.

Spring-8. Incident beams from an undulator were monochromatized to $\lambda = 0.63582 \text{ \AA}$ with rotated inclined Si(111) double crystal monochromators. The sample was sealed in a borosilicate glass capillary tube with an inner diameter of 1.0 mm and rotated at a speed of 6.3 rad/s. The synchrotron XRD data were collected in a 2θ range from 1.5° to 30.0° with a step interval of 0.004° and a counting time of 2.0 s per step.

Results and Discussion

Absorption and Fluorescence Spectra in Solution. Absorption and emission maxima (λ_{abs} and λ_{em} , respectively) of DPHs **1–10** in toluene solution are summarized in Table 1. Depending on the nature of substituents, λ_{em} changed in the range 428–491 nm. The spectra for some of the DPH derivatives in low polar solvents are already reported.^{5,22} The fluorescence spectra in toluene showed vibrational structures with spacings of 1200–1400 cm^{-1} , corresponding to the C=C and C–C stretches of conjugated polyenes. Similar spacings were also observed in the absorption spectra. The spectral features in solution are considered to be characteristic of monomer fluorescence.

Figure 1A shows plots of λ_{em}^{-1} and $\lambda_{\text{abs}}^{-1}$ versus ¹H NMR chemical shift of the peaks for triene 1-H and 6-H protons in solution. The data for compound **7** are not included in the figure, because its NMR spectrum was not obtained due to low solubility. The NMR chemical shift correlated well with the electron-donating or -withdrawing nature of ring-substituents. Electron-donating groups increased the electron density of the hexatriene moiety and moved the peaks to higher magnetic fields, whereas electron-withdrawing groups induced the shifts to lower magnetic fields. As seen in the figure, λ_{em}^{-1} and $\lambda_{\text{abs}}^{-1}$ correlated well with the chemical shifts. The dependences of λ_{em}^{-1} and $\lambda_{\text{abs}}^{-1}$ on substituents were similar, which is in accordance with the fact that both these values roughly correspond to the energy of the 0–0 transition. Strong electron-donating or -withdrawing substituents decreased λ_{em}^{-1} and $\lambda_{\text{abs}}^{-1}$ values. Introduction of these substituents on the benzene ring leads to more complete π -electron delocalization throughout the molecule. Thus, the observed red shifts in λ_{em} and λ_{abs} can be ascribed to the extended π -conjugation of the derivatives with strong electron-donating or -withdrawing substituents.

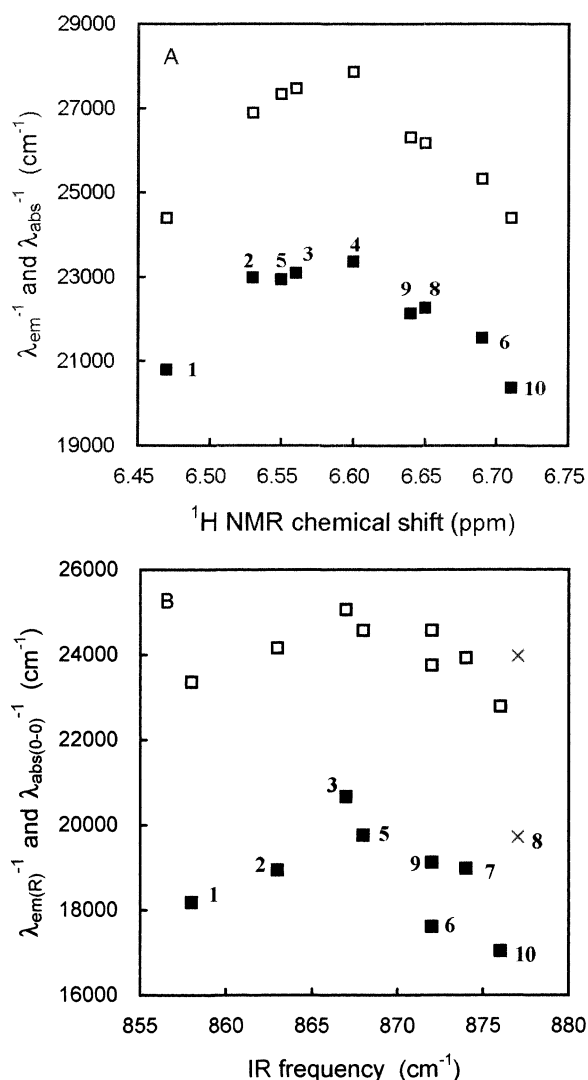


Figure 1. (A) Plots of λ_{em}^{-1} and λ_{abs}^{-1} in toluene vs ^1H NMR chemical shift for the triene 1-H and 6-H protons in chloroform- d . (B) Plots of $\lambda_{em(R)}^{-1}$ and $\lambda_{abs(0-0)}^{-1}$ vs IR frequency of the C–H out-of-plane bending vibration of *para*-substituted benzene rings for DPHs in microcrystals.

TABLE 2: Melting Points and Absorption and Emission Properties of Diphenylhexatrienes in Microcrystals

compd	R =	mp (°C)	$\lambda_{abs(0-0)}$ (nm)	$\lambda_{em(0-0)}$ (nm)	$\lambda_{em(R)}$ (nm)	ϕ_{flu}
1	NMe ₂	247	428	not observed	550	0.005
2	OMe	250	414	464	528	0.008
3	Me	208	399	449	484	0.095
4	H	196	398	444	463	0.14
5	Cl	218	407	460	506	0.015
6	CHO	214	421	not observed	568	0.002
7	COOH	>300	418	494 (shoulder)	527	0.006
8	COOMe	251	417	478	507	0.18
9	CN	224	407	458 (very weak)	523	0.002
10	NO ₂	229	439	not observed	587	0.013

Absorption and Fluorescence Spectra in Microcrystals and Thin Films. In the solid-state DPHs, peaks due to the 0–0 transition and/or red-shifted main bands were observed in fluorescence spectra. Table 2 lists $\lambda_{abs(0-0)}$, $\lambda_{em(0-0)}$, and $\lambda_{em(R)}$ for the microcrystals of 1–10. The position of $\lambda_{abs(0-0)}$ was determined from the highest π – π^* transition peak in the absorption spectrum. The position of $\lambda_{em(0-0)}$ was the fluorescence maximum of the 0–0 transition band (the maximum of “monomer fluorescence”), and $\lambda_{em(R)}$ was determined from the

peak at shortest wavelength in the main red-shifted band. It should be noted, however, that the $\lambda_{em(R)}$ values for derivatives 3, 4, and 8 shown in Table 2 are approximate values, since the “red-shifted” main bands were overlapped with vibrational progressions of strong 0–0 transition bands for these compounds. It is found that $\lambda_{abs(0-0)}$ and $\lambda_{em(0-0)}$ shifted to longer wavelengths from λ_{abs} and λ_{em} in solution (Table 1), respectively. The red shifts can be attributed to the higher dielectric polarizability of the crystalline environment.

By introduction of various substituents, $\lambda_{em(R)}$ values for the microcrystals were tuned in the visible spectral range 463–587 nm. The microcrystals of the derivatives with strong electron-donating or -withdrawing substituents, 1 and 10, showed the most red-shifted fluorescence among the derivatives studied, as seen in Table 2. As expected, $\lambda_{em(R)}$ for 4 was the shortest among those for the DPHs used in this study.

The spectral features of the solid-state fluorescence were strongly dependent on substituents, in contrast to the observations in solution. The spectra for the derivatives 3, 4, and 8 showed clear structures with strong 0–0 bands. The spectra of 5 and 7 were only weakly structured with moderately red-shifted main bands. For the derivatives with increased electron-donating strengths of substituents, the main bands moved to longer wavelengths and exhibited vibrational structures, as observed for 1 and 2. For the derivatives with strong electron-withdrawing groups such as 6, 9, and 10, on the other hand, the main red-shifted bands were structureless. The 0–0 transition was not observed or only weakly observed. A similar broad spectrum is reported for the nanoparticles of the *p,p'*-dicyano-substituted PV oligomer with three benzene rings.¹⁰ However, it should be noted that ester 8 is rather exceptional. Although methoxycarbonyl is a considerably strong electron-withdrawing group, it showed a structured fluorescence spectrum. The intensity of the 0–0 band was strong, and the main band was observed in a relatively short wavelength region (Table 2). This may possibly be due to the very different crystal structure of the compound.

Figure 1B shows plots of $\lambda_{em(R)}^{-1}$ and $\lambda_{abs(0-0)}^{-1}$ versus IR frequency of C–H out-of-plane bending (or wag) vibrations of *p*-substituted benzene rings for DPHs in microcrystals. For monosubstituted benzenes, it is known that the wavenumber of this 900 cm^{-1} phenyl band is highly sensitive to substituents.²³ It correlates very well with the electron-donating or -withdrawing characteristics of the substituents; electron-withdrawing groups such as nitro raise the frequency, while electron-donating groups such as dimethylamino lower the frequency. For the present DPH derivatives, a similar substituent dependence of the IR frequency was observed. As seen in the figure, $\lambda_{em(R)}^{-1}$ and $\lambda_{abs(0-0)}^{-1}$ correlated well with the IR frequencies, although compound 8 seemed to be somewhat exceptional, as described above. Values of $\lambda_{em(R)}^{-1}$ and $\lambda_{abs(0-0)}^{-1}$ decreased with increasing strengths of the electron-donating or -withdrawing natures of substituents. Compound 4 is not included in the figure due to its different ring-substitution pattern. Considering that $\lambda_{em(R)}^{-1}$ for 4 (22 500 cm^{-1}) is above the value for 3, it can be said that values of $\lambda_{em(R)}^{-1}$ are more strongly dependent on substituents than those of $\lambda_{abs(0-0)}^{-1}$ (and $\lambda_{em(0-0)}^{-1}$, not shown in Figure 1B). This suggests that the main red-shifted band is the emission from excited states that are different from those produced by 0–0 absorption processes, such as excimers or excited states of oriented aggregates. From the strong dependence of $\lambda_{em(R)}$ on substituents, it is probable that charge transfer (CT) type intermolecular interactions induced by substituents play an important role in the formation of the excimers and aggregates.

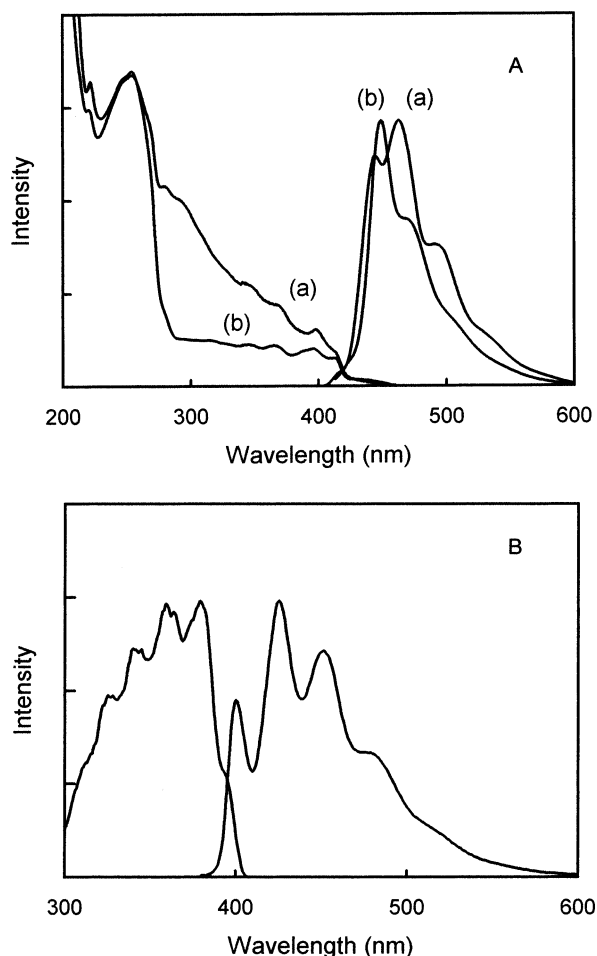


Figure 2. (A) Absorption and fluorescence spectra of **4** in (a) microcrystals and (b) a vacuum deposited film. (B) Fluorescence and excitation spectra of **4** in ether glass at 77 K. Excitation and emission wavelengths were $E_X = 360$ nm and $E_M = 450$ nm, respectively.

The triene-phenyl π -system will serve as either electron-donating or -withdrawing groups, depending on the nature of substituents.

It is also found that $\lambda_{em(R)}^{-1}$ values correlate considerably well with melting points (Table 2). Compounds having higher melting points showed $\lambda_{em(R)}$ at longer wavelengths. Since melting points are directly connected with the strengths of intermolecular interactions in the solid state, the results indicate that strong intermolecular interactions lead to the decrease in the energy levels of excited states that are involved in the emission processes for these compounds.

Unsubstituted Derivative 4. Figure 2A-(a) shows the absorption and fluorescence spectra for the microcrystals of **4**. The fluorescence spectrum showed a vibrational structure with peaks at 444, 463, 491, and 532 nm. Figure 2A-(b) shows the spectra of **4** in a vacuum deposited thin film. The fluorescence spectrum for the deposited film was structured similarly with peaks at 449, 471, 509, and 547 nm. The intensity of the highest energetic peak around 415 nm for the microcrystals and thin film was strongly reduced, probably due to reabsorption. However, we cannot exclude the possibility that these weak peaks are at least partially due to the transition from S_2 to S_0 , since weak emissions at shorter wavelengths observed for DPHs in low polarity solvents are assigned to the S_2 - S_0 transition.²² The absorption maxima for the microcrystals and thin film were observed at 398 nm. Figure 2B shows the excitation and fluorescence spectra of **4** in ether glass at 77 K. The fluorescence

spectrum showed a clear structure with peaks at 400, 425, 451, 479, and 520 nm. In the excitation spectrum, a peak maximum was located at 380 nm. The mirror image relationship was seen between the excitation and emission spectra. It can be seen from Figure 2A and B that 0-0 transition bands are strongly observed for the microcrystals and thin film, and the "red-shifted" main bands in Figure 2A are largely overlapped with the vibrational progressions of the strong 0-0 bands.

Methoxy Derivative 2. Figure 3A shows the absorption, excitation, and fluorescence spectra of **2** in a vacuum deposited film. In the main part of the fluorescence spectrum (F_1), peaks were observed at 513, 550, and 594 nm. The peaks at 550 and 594 nm should be a vibrational progression of the peak at 513 nm. The spacing is 1330 cm^{-1} , which is similar to the value in toluene. In the shorter wavelength region of the spectrum (F_2), weak peaks were observed at 439 and 462 nm. Figure 3C shows the excitation and emission spectra of **2** in ether at 77 K. The fluorescence spectrum showed a clear vibrational structure, and the positions of the peaks at 410, 435, 461, and 496 nm were very similar to those in solution. The excitation and emission spectra show mirror symmetry. The emission at 77 K should therefore be the monomer fluorescence in the solid state. By comparing the fluorescence spectrum for the thin film with that in ether at low temperature, F_2 in Figure 3A can be assigned to the monomer fluorescence. The main spectrum F_1 was, on the other hand, clearly structured and significantly red-shifted from the monomer fluorescence, suggesting that it is the emission from ground-state aggregates. The formation of ground-state aggregates in the solid state has also been assumed for PV oligomers^{8-10,13} and 1,4-diphenyl-1,3-butadienes.²⁴ In the absorption spectrum for the thin film of **2**, peaks were observed at 427 nm, 415 nm (A_2 in Figure 3A), and 308 nm. Since the mirror image relationship was observed between A_2 and F_2 , A_2 peaks are probably due to a monomeric species. On the other hand, the origin of F_1 could not be determined in the absorption spectrum. However, in addition to the strong peaks at 411 and 427 nm, its excitation spectrum showed weak peaks at 464 and 500 nm (A_1 in Figure 3A), which might be the origin of F_1 . It is not clear why A_1 was not clearly seen in the absorption spectrum; however, this is possibly because the peaks were too weak to be observed.

Oelkrug et al. have reported the absorption and fluorescence spectra for the nanoaggregates of oligo-PVs.¹³ The high stationary fluorescence anisotropies observed for these compounds are attributed to a high degree of molecular alignment in the aggregates. The spectra are interpreted mainly on the basis of the molecular exciton model, and the shifts in the spectral band positions from solution data are considered to be an indirect evidence for molecular orientation in the solid state. In the present study, it is found that the shape of the fluorescence spectrum for the thin film of **2** is similar to those for the nanoaggregates of unsubstituted oligo-PVs. In Figure 3A, the main fluorescence peak at 513 nm was red-shifted by 2150 cm^{-1} from the 0-0 origin (monomer emission) at 462 nm. The absorption at 415 nm was red-shifted by 2800 cm^{-1} from the 0-0 origin in toluene solution at 372 nm, whereas the absorption at 308 nm was strongly blue-shifted by 5600 cm^{-1} from the origin. These spectral shifts for **2** are similar to the corresponding values reported for the oligo-PV nanoaggregates, suggesting the formation of "highly oriented aggregates" in the thin film of **2**.

Interestingly, the fluorescence spectrum for the deposited film of **2** showed a close resemblance to that for the thin film of high molecular weight PPV. Figure 4 shows the absorption and fluorescence spectra of a PPV thin film. The fluorescence

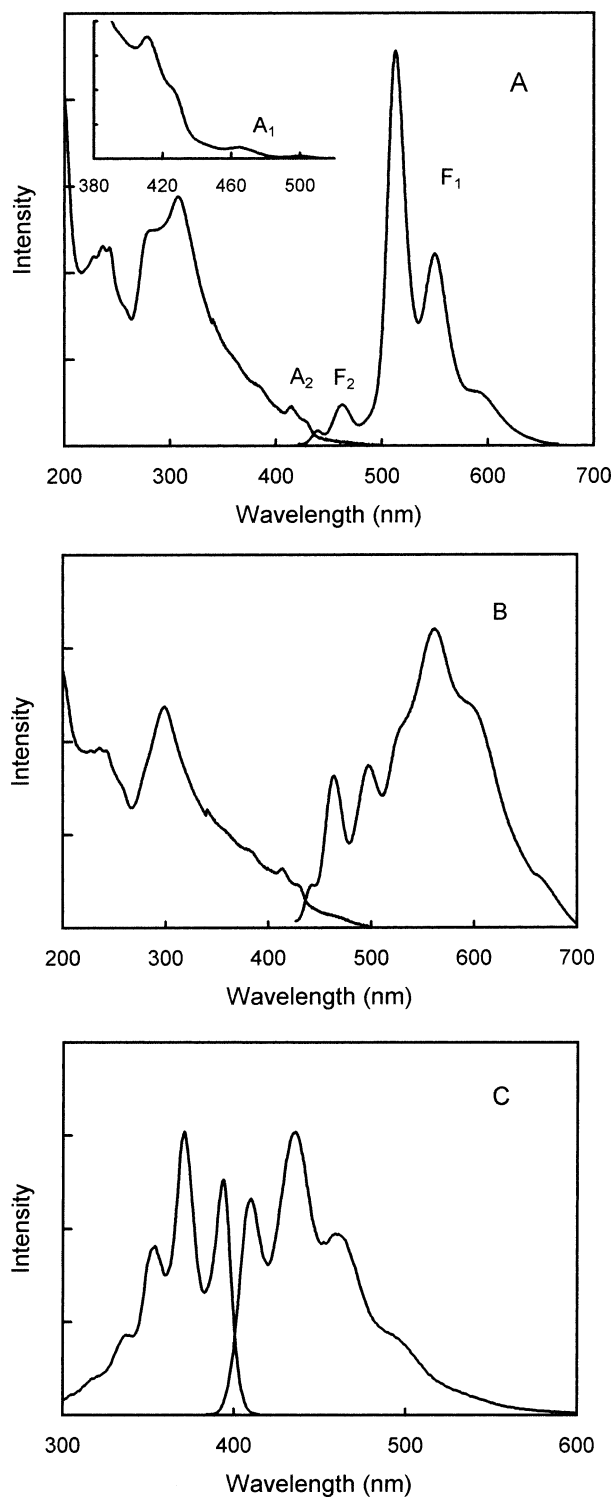


Figure 3. Absorption and fluorescence spectra of **2** in (A) a vacuum deposited film and (B) microcrystals. Inset in part A: excitation spectrum for the deposited film. $E_X = 375$ nm and $E_M = 596$ nm. C) Fluorescence and excitation spectra of **2** in ether at 77 K. $E_X = 360$ nm and $E_M = 460$ nm.

spectrum is in good agreement with that reported in the literature.²⁵ The positions of the fluorescence peaks at 518, 556, and 603 nm were very similar to those of F_1 for **2**. Furthermore, the absorptions at 463 and 496 nm for PPV were observed at quite similar wavelengths to that of A_1 in the excitation spectrum of **2**. The observation implies that the aggregates of the low molecular weight compound **2** possess similar effective π -conjugation lengths (ECLs) in the excited state to those for the

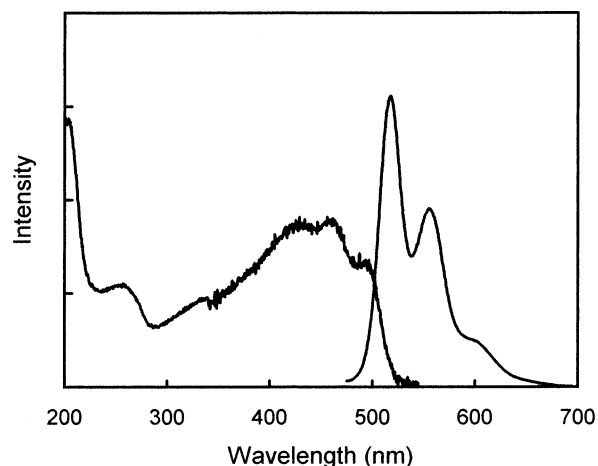


Figure 4. Absorption and fluorescence spectra of a PPV thin film.

high polymer PPV. The ECL for high molecular weight PPV prepared via the precursor route is spectroscopically estimated to be 10–17 repeating units.²⁶ It is possible, therefore, that the oriented aggregates of **2** are formed in the solid state by overlapping of adjacent **2** molecules with, for example, Ar—CH=CH—CH=CH— moieties. In the thin film of **2**, π -electrons may be delocalized in the supramolecular structures formed by simple intermolecular interactions. The influence of through-space interactions between two oligo-PV chromophores in close proximity on the optical spectra has been recently investigated using [2,2]paracyclophane compounds.²⁷

Figure 3B shows the spectra of **2** in microcrystals. The spectral features were rather complex, probably due to the structural inhomogeneity of the microcrystalline sample. The emissions at 441, 464, and 498 nm are due to a monomeric species. The main red-shifted spectrum in the region 500–700 nm was weakly structured. The peak positions at 528, 561, and 601 nm were similar to those for the thin film, suggesting that the spectrum for the microcrystals is the overlap of a structured emission due to ground-state aggregates and a broad one around 560 nm. The broad emission, which was not observed for the deposited film, may be due to an excimer, local structural defects, and/or an impurity trap in the microcrystals.

Single crystals of high quality for X-ray analysis are not obtained at present. However, 2D ^1H exchange NMR measurements of **2** in the solid state revealed that a hexatriene chain was located close to a methoxy group of an adjacent molecule in microcrystals. The ^1H CRAMPS spectrum showed peaks at δ 5.8 (aromatic protons), 5.1 and 4.4 (triene protons), and 3.1 (methoxy protons). In the 2D ^1H exchange spectra, the cross-peaks of olefinic and methoxy protons in addition to diagonal peaks were observed, indicating the nearness of the triene and methoxy groups. Although we cannot conclude the formation of the oriented aggregates at present due to the lack of crystal data, the partially overlapping structure is thus supported from the solid-state NMR measurements.

***N,N*-Dimethylamino Derivative 1.** Figure 5 shows the absorption and fluorescence spectra for the microcrystals of **1**. Fluorescence peaks were observed at 550, 591, 628, and 671 nm. The solid-state fluorescence was largely red-shifted from the monomer fluorescence in solution (Table 1). Similar to the case of **2**, the emission spectrum of **1** showed weak structures, which is possibly due to the formation of ground-state aggregates in the solid state. Unlike the case of **2**, however, no monomer emission was observed for the microcrystals of **1**.

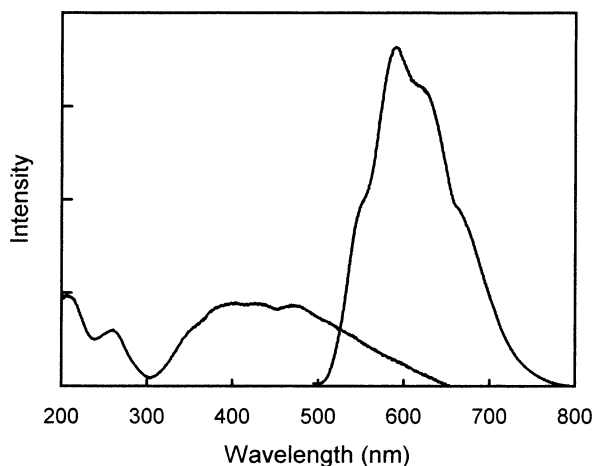


Figure 5. Absorption and fluorescence spectra of **1** in microcrystals.

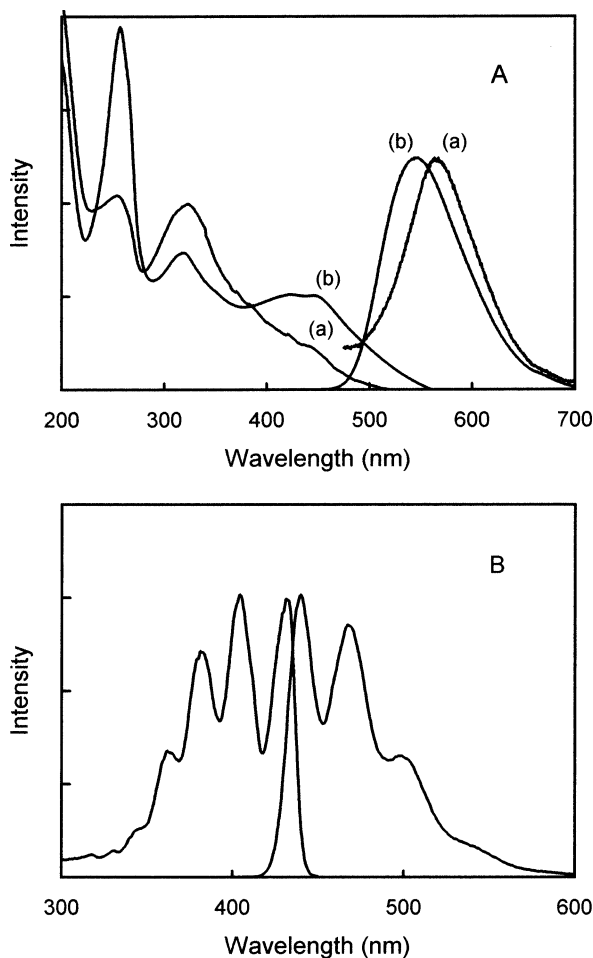


Figure 6. (A) Absorption and fluorescence spectra of **6** in (a) microcrystals and (b) a vacuum deposited film. (B) Fluorescence and excitation spectra of **6** in ether at 77 K. $E_X = 375$ nm and $E_M = 470$ nm.

Formyl Derivative 6. Figure 6A-(a) shows the absorption and fluorescence spectra for the microcrystals of **6**. The fluorescence spectrum was broad and structureless. The maximum was observed at 568 nm, which shifted to longer wavelengths by 100 nm from that for the monomer fluorescence in solution. Figure 6A-(b) shows the spectra of **6** in a vacuum deposited film. The absorption and emission maxima were observed at 423 and 546 nm, respectively. The thin film sample showed a slight red-shift in absorption and a small blue shift in

emission relative to those for the microcrystals. Figure 6B shows the excitation and fluorescence spectra of **6** in ether at 77 K. The spectrum at 77 K showed a distinct vibrational structure, which is different from the broad fluorescence for the microcrystals and deposited film. The emission maximum was observed at 440 nm, and the maximum peak in the excitation spectrum was located at 431 nm. The excitation and emission spectra showed the mirror image relationship. The fluorescence spectrum is similar to that in toluene solution, showing the emission at 77 K to be the monomer fluorescence in the solid state. From the broad spectral features and large red-shifts from the monomer fluorescence, the fluorescence spectra of **6** in microcrystals and deposited film can be assigned to excimer emission.

The XRD pattern of sample **6** showed considerably anisotropic broadening reflections in the region $9^\circ < 2\theta < 12^\circ$. In this analysis, the structural model could not be determined completely, because a large number of reflections were overlapped due to the anisotropic broadening. Indexing of reflections with DICVOL91 gave an orthorhombic unit cell of $a = 30.1739(7)$ Å, $b = 12.5921(2)$ Å, $c = 3.98392(11)$ Å, $V = 1513.70$ Å³, and $Z = 4$ with acceptable figures of merit: $F_{25} = 222$ and $M_{25} = 37$. Reflection conditions derived from the indexed reflections were $h + l = 2n$ for $h0l$, $h = 2n$ for $h00$, $k = 2n$ for $0k0$, and $l = 2n$ for $00l$, affording space group $P21/n$ (No. 14). Observed integrated intensities, $|F_o|^2$, of 859 reflections in the region $d > 1.22$ Å were extracted by the Le Bail method²⁸ with a versatile pattern-fitting system RIETAN-2000.²⁹ Partial profile relaxation²⁹ with a modified split pseudo-Voigt function was applied to 11 anisotropic broadening reflections, which significantly improved fits between their observed and calculated profiles. Although the integral intensities of the overlapped reflections could not be estimated adequately, a preliminary structural model was obtained from the $|F_o|^2$ values by a direct method using SIRPOW97 in EXPO.³⁰

It is revealed that two molecules of **6** lie parallel along the c axis to form a face-to-face pair, which is in agreement with the formation of excimer. The shortest intermolecular distance between hexatrienes is shown to be 3.4–3.6 Å. For the solid-state $[2 + 2]$ photocycloadditions, it is well-known that the distance between the potentially reactive double bonds should be < 4.2 Å.³¹ In fact, **6** undergoes intermolecular $[2 + 2]$ cycloaddition at the 1,2-positions of the triene to give a mirror symmetric dimer when irradiated in the solid state.⁶

The positions of aromatic carbons and formyl groups in the unit cell could not be determined unequivocally from the XRD data due to the very limited number of observed reflections. However, ¹³C CP/MAS NMR and IR spectra clearly indicated the presence of intermolecular C–H \cdots O hydrogen bonds involving the aldehyde C=O groups.⁶ The ¹H CRAMPS spectrum gave peaks at δ 9.3 (aldehyde protons), 6.7 (aromatic protons), and 5.8 (triene protons and a part of aromatic protons). The 2D ¹H exchange NMR spectra showed strong cross-peaks between 9.3 and 6.7 ppm peaks and rather weak cross-peaks between 9.3 and 5.8 ppm peaks, suggesting that the C=O groups formed hydrogen bonds not with the hexatriene protons but with the aromatic or formyl protons.

In liquid paraffin, a structured spectrum was observed in the region 440–480 nm in addition to a broad one around 560 nm due to the inhomogeneous nature of the sample. The relative intensity of the peak at 560 nm to that at 460 nm increased as the concentration of **6** increased, which is consistent with the peak assignment described above. The fluorescence of **6** was thus largely red-shifted relative to that for the unsubstituted

parent compound. The red-shift was rather unexpected, since only a few examples have been reported for the effects of formyl substitution on the solid-state emission properties of aromatic compounds.³²

Fluorescence Emission Efficiencies. In low polarity solvents such as toluene, ϕ_{flu} values for DPHs were in general high (Table 1). The low ϕ_{flu} values for **7** and **10** are due to efficient *cis*–*trans*-photoisomerization in methanol solvent and singlet–triplet intersystem crossing resulting from nitro substitution,⁵ respectively.

Table 2 shows the values of ϕ_{flu} in the solid state. As seen in the table, the emission efficiencies of DPHs in microcrystals were strongly dependent on substituents and were considerably lower than those in toluene solution. The low ϕ_{flu} can be attributed to efficient nonradiative decay processes due to strong intermolecular interactions in the solid state. Among the DPHs used in this study, **3**, **4**, and **8**, which are photostable in the solid state, showed relatively high values of ϕ_{flu} . On the other hand, ϕ_{flu} values for **6** and **9** were very low, corresponding to the high photoreactivity in the solid state.⁶ Although the emission spectrum for the thin film of **2** was quite similar to that for the PPV film, ϕ_{flu} for **2** was found to be considerably lower than the value for PPV ($\phi_{\text{flu}} = 0.04$ – 0.05).²⁵ Since the molecules of **2** in the ground-state aggregates are considered to be in a tight coplanar arrangement, nonradiative processes are expected to be strongly induced by intermolecular interactions.

Fluorescence Lifetimes. Values of τ_s for the toluene solutions of DPHs were measured to be 2–5 ns by the single photon counting method. For example, the τ_s values were 2.4, 5.2, and 2.1 ns for compounds **2**, **4**, and **6**, respectively. For most of the derivatives, fluorescence decay curves were single exponential, indicating the homogeneous nature of fluorescent species in dilute solution. In the case of **10**, however, biexponential fitting gave better fits. This decay behavior has been explained in terms of an additional excited state, which is formed by intramolecular charge transfer from the triene-phenyl π -system to the nitro group.⁵

Fluorescence decay curves were also measured for the deposited thin films of **2**, **4**, and **6**, since τ_s measurements would provide important insight into the fluorescent excited states such as excimers and excited states of aggregates. In contrast to the observations in solution, however, the decay curves were very nonexponential. The curves showed a fast initial decay followed by a much slower decrease. Biexponential fitting gave short τ_s < 200 ps (90–95%) and relatively long $\tau_s \sim 10$ ns (5–10%).

Conclusions

Fluorescence spectra for the microcrystals and thin films of DPHs **1**–**10** are strongly dependent on substituents. Positions of $\lambda_{\text{em(R)}}$ are tuned in the range of 463–587 nm by introduction of various substituents. They shift to red as the strength of the electron-donating/withdrawing substituents on the ring increases. The strong substituent dependence of the solid-state fluorescence relative to that in solution can be attributed to strong CT type intermolecular interactions induced by substituents. The structured and red-shifted spectrum for **2** is possibly due to the formation of oriented aggregates in the ground state. The fluorescence spectrum for the thin film of **2** shows a close resemblance to that for the PPV thin film, which implies similar ECLs in the excited state for the aggregates of **2** and PPV. The fluorescence spectrum for the microcrystals of **1** is similarly red-shifted and structured. The fluorescence spectra for the derivatives with strong electron-withdrawing groups are red-

shifted and structureless. The fluorescence of **6** is assigned to excimer emission.

References and Notes

- (1) Allen, M. T.; Miola, L.; Whitten, D. G. *J. Am. Chem. Soc.* **1988**, *110*, 3198. (b) Trotter, P. J.; Storch, J. *Biochim. Biophys. Acta* **1989**, *982*, 131.
- (2) Allen, M. T.; Whitten, D. G. *Chem. Rev.* **1989**, *89*, 1691.
- (3) Sonoda, Y.; Kaeriyama, K. *Polymer* **1992**, *33*, 2437. (b) Sonoda, Y.; Suzuki, Y. *J. Chem. Soc., Perkin Trans. 2* **1996**, 401. (c) Sonoda, Y.; Suzuki, Y. *Chem. Lett.* **1996**, 659. (d) Sonoda, Y.; Morii, H.; Sakuragi, M.; Suzuki, Y. *Chem. Lett.* **1998**, 349. (e) Sonoda, Y.; Kawanishi, Y.; Sakuragi, M. *Chem. Lett.* **1999**, 587.
- (4) Saltiel, J.; Ko, D.-H.; Fleming, S. A. *J. Am. Chem. Soc.* **1994**, *116*, 4099. (b) Saltiel, J.; Wang, S.; Ko, D.-H.; Gormin, D. A. *J. Phys. Chem. A* **1998**, *102*, 5383. (c) Saltiel, J.; Crowder, J. M.; Wang, S. *J. Am. Chem. Soc.* **1999**, *121*, 895. (d) Saltiel, J.; Wang, S.; Watkins, L. P.; Ko, D.-H. *J. Phys. Chem. A* **2000**, *104*, 11443.
- (5) Sonoda, Y.; Kwok, W. M.; Petrusek, Z.; Ostler, R.; Matousek, P.; Towrie, M.; Parker, A. W.; Phillips, D. J. *Chem. Soc., Perkin Trans. 2* **2001**, 308.
- (6) Sonoda, Y.; Miyazawa, A.; Hayashi, S.; Sakuragi, M. *Chem. Lett.* **2001**, 410.
- (7) Kraft, A.; Grimsdale, A. C.; Holmes, A. B. *Angew. Chem., Int. Ed.* **1998**, *37*, 403.
- (8) Oelkrug, D.; Tompert, A.; Gierschner, J.; Egelhaaf, H.-J.; Hanack, M.; Hohloch, M.; Steinhuber, E. *J. Phys. Chem. B* **1998**, *102*, 1902.
- (9) Strehmel, B.; Sarker, A. M.; Malpert, J. H.; Strehmel, V.; Seifert, H.; Neckers, D. C. *J. Am. Chem. Soc.* **1999**, *121*, 1226.
- (10) Schweikart, K.-H.; Hohloch, M.; Steinhuber, E.; Hanack, M.; Lüer, L.; Gierschner, J.; Egelhaaf, H.-J.; Oelkrug, D. *Synth. Met.* **2001**, *121*, 1641.
- (11) Brouwer, H. J.; Krasnikov, V. V.; Pham, T. A.; Gill, R. E.; van Hutten, P. F.; Hadzioannou, G. *Chem. Phys.* **1998**, *227*, 65.
- (12) Gill, R. E.; Hilberer, A.; van Hutten, P. F.; Berentschot, G.; Werts, M. P. L.; Meetsma, A.; Wittmann, J.-C.; Hadzioannou, G. *Synth. Met.* **1997**, *84*, 637. (b) Döttinger, S. E.; Hohloch, M.; Hohnholz, D.; Segura, J. L.; Steinhuber, E.; Hanack, M. *Synth. Met.* **1997**, *84*, 267. (c) van Hutten, P. F.; Krasnikov, V. V.; Hadzioannou, G. *Acc. Chem. Res.* **1999**, *32*, 257.
- (13) Egelhaaf, H.-J.; Gierschner, J.; Oelkrug, D. *Synth. Met.* **1996**, *83*, 221. (b) Oelkrug, D.; Egelhaaf, H.-J.; Gierschner, J.; Tompert, A. *Synth. Met.* **1996**, *76*, 249. (c) Gierschner, J.; Egelhaaf, H.-J.; Oelkrug, D. *Synth. Met.* **1997**, *84*, 529.
- (14) Sassella, A.; Borghesi, A.; Meinardi, F.; Tubino, R.; Gurioli, M.; Botta, C.; Porzio, W.; Barbarella, G. *Phys. Rev. B* **2000**, *62*, 11170. (b) Hotta, S.; Ichino, Y.; Yoshida, Y.; Yoshida, M. *J. Phys. Chem. B* **2000**, *104*, 10316. (c) Iannotta, S.; Toccoli, T.; Boschetti, A.; Scardi, P. *Synth. Met.* **2001**, *122*, 221. (d) Tavazzi, S.; Meinardi, F.; Borghesi, A.; Sassella, A.; Tubino, R. *Synth. Met.* **2001**, *124*, 71. (e) Botta, C.; Destri, S.; Porzio, W.; Bongiovanni, G.; Loi, M. A.; Mura, A.; Tubino, R. *Synth. Met.* **2001**, *122*, 395. (f) Sassella, A.; Borghesi, A.; Meinardi, F.; Riva, D.; Tavazzi, S.; Tubino, R.; Porzio, W.; Destri, S.; Barbarella, G.; Garnier, F. *Synth. Met.* **2001**, *116*, 213.
- (15) Cornil, J.; dos Santos, D. A.; Crispin, X.; Silbey, R.; Brédas, J. L. *J. Am. Chem. Soc.* **1998**, *120*, 1289. (b) Beljonne, D.; Cornil, J.; Silbey, R.; Millié, P.; Brédas, J. L. *J. Chem. Phys.* **2000**, *112*, 4749.
- (16) Cornil, J.; dos Santos, D. A.; Beljonne, D.; Brédas, J. L. *J. Phys. Chem.* **1995**, *99*, 5604. (b) Cornil, J.; Beljonne, D.; dos Santos, D. A.; Brédas, J. L. *Synth. Met.* **1996**, *76*, 101. (c) dos Santos, D. A.; Beljonne, D.; Cornil, J.; Brédas, J. L. *Chem. Phys.* **1998**, *227*, 1.
- (17) Spangler, C. W.; McCoy, R. K.; Dembek, A. A.; Sapochak, L. S.; Gates, B. D. *J. Chem. Soc., Perkin Trans. 1* **1989**, 151. (b) Spangler, C. W.; Hall, T. J.; Havelka, K. O.; Polis, D. W.; Sapochak, L. S.; Dalton, L. R. *Proc. SPIE-Int. Soc. Opt. Eng.* **1990**, *1337*, 125.
- (18) Murase, I.; Ohnishi, T.; Noguchi, T.; Hirooka, M. *Polym. Commun.* **1984**, *25*, 327. (b) Sonoda, Y.; Kaeriyama, K. *Bull. Chem. Soc. Jpn.* **1992**, *65*, 853.
- (19) Birks, J. B.; Kazzaz, A. A.; King, T. A. *Proc. R. Soc. (London)* **1966**, *A291*, 556.
- (20) Burum, D. P.; Cory, D. G.; Gleason, K. K.; Levy, D.; Bielecki, A. *J. Magn. Reson., Ser. A* **1993**, *104*, 347.
- (21) Caravatti, P.; Neuenschwander, P.; Ernst, R. R. *Macromolecules* **1985**, *18*, 119.
- (22) Alford, P. C.; Palmer, T. F. *Chem. Phys. Lett.* **1982**, *86*, 248. (b) Alford, P. C.; Palmer, T. F. *J. Chem. Soc., Faraday Trans. 2* **1983**, *79*, 433.

- (23) Lin-Vien, D.; Colthup, N. B.; Fateley, W. G.; Grasselli, J. G. *The Handbook of Infrared and Raman Characteristic Frequencies of Organic Molecules*; Academic Press Inc.: San Diego, CA, 1991; pp 284–287. (b) Colthup, N. B. *Appl. Spectrosc.* **1976**, *30*, 589.
- (24) Singh, A. K.; Krishna, T. S. R. *J. Phys. Chem. A* **1997**, *101*, 3066.
- (25) Köpping-Grem, G.; Leising, G.; Schimetta, M.; Stelzer, F.; Huber, A. *Synth. Met.* **1996**, *76*, 53.
- (26) Woo, H. S.; Lhost, O.; Graham, S. C.; Bradley, D. D. C.; Friend, R. H.; Quattrocchi, C.; Brédas, J. L.; Schenk, R.; Müllen, K. *Synth. Met.* **1993**, *59*, 13.
- (27) Bartholomew, G. P.; Bazan, G. C. *Acc. Chem. Res.* **2001**, *34*, 30.
- (28) Le Bail, A.; Duroy, H.; Fourquet, J. L. *Mater. Res. Bull.* **1988**, *23*, 447.
- (29) Izumi, F.; Ikeda, T. *Mater. Sci. Forum* **2000**, *321–324*, 198.
- (30) Altomare, A.; Burla, M. C.; Camalli, M.; Carrozzini, B.; Cascarano, G. L.; Giacovazzo, C.; Guagliardi, A.; Moliterni, A. G. G.; Polidori, G.; Rizzi, R. *J. Appl. Crystallogr.* **1999**, *32*, 339.
- (31) Ramamurthy, V.; Venkatesan, K. *Chem. Rev.* **1987**, *87*, 433.
- (32) Yanai, H.; Yoshizawa, D.; Tanaka, S.; Fukuda, T.; Akazome, M.; Ogura, K. *Chem. Lett.*, **2000**, 238.